

Communication

Spatiotemporal Rainfall Trends in the Brazilian Legal Amazon between the Years 1998 and 2015

Celso H. L. Silva Junior ^{1,*}, Catherine T. Almeida ¹, Jessflan R. N. Santos ²,
Liana O. Anderson ³, Luiz E. O. C. Aragão ^{1,4} and Fabrício B. Silva ²

¹ Tropical Ecosystems and Environmental Sciences Laboratory (TREES), Remote Sensing Division, National Institute for Space Research-INPE, São José dos Campos 12227-010 SP, Brazil; cathe.torres@gmail.com (C.T.A.); luiz.aragao@inpe.br (L.E.O.C.A.)

² Masters in Environment, Ceuma University—UniCEUMA, São Luís 65075-120 MA, Brazil; jessflan@ymail.com (J.R.N.S); fabricioagro@gmail.com (F.B.S.)

³ National Center for Monitoring and Early Warning of Natural Disasters—CEMADEN, São José dos Campos 12247-016 SP, Brazil; liana.anderson@cemaden.gov.br

⁴ College of Life and Environmental Sciences, University of Exeter, Exeter EX4 4RJ, UK

* Correspondence: celso.junior@inpe.br; Tel.: +55-12-3208-6425

Received: 1 June 2018; Accepted: 7 September 2018; Published: 10 September 2018



Abstract: Tropical forests play an important role as a reservoir of carbon and biodiversity, specifically forests in the Brazilian Amazon. However, the last decades have been marked by important changes in the Amazon, particularly those associated with climatic extremes. Quantifying the variability of rainfall patterns, hence, is essential for understanding changes and impacts of climate upon this ecosystem. The aim of this study was to analyse spatiotemporal trends in rainfall along the Brazilian Legal Amazon between 1998 and 2015. For this purpose, rainfall data derived from the Tropical Rainfall Measuring Mission satellite (TRMM) and nonparametric statistical methods, such as Mann–Kendall and Sen’s Slope, were used. Through this approach, some patterns were identified. No evidence of significant rainfall trends ($p \leq 0.05$) for annual or monthly (except for September, which showed a significant negative trend) averages was found. However, significant monthly negative rainfall anomalies were found in 1998, 2005, 2010, and 2015, and positive in 1999, 2000, 2004, 2009, and 2013. The annual pixel-by-pixel analysis showed that 92.3% of the Brazilian Amazon had no rainfall trend during the period analysed, 4.2% had significant negative trends ($p \leq 0.05$), and another 3.5% had significant positive trends ($p \leq 0.05$). Despite no clear temporal rainfall trends for most of the Amazon had negative trends for September, corresponding to the peak of dry season in the majority of the region, and negative rainfall anomalies found in 22% of the years analysed, which indicate that water-dependent ecological processes may be negatively affected. Moreover, these processes may be under increased risk of disruption resulting from other drought-related events, such as wildfires, which are expect to be intensified by rainfall reduction during the Amazonian dry season.

Keywords: amazon forest; droughts; floods; Mann–Kendall test; TRMM

1. Introduction

Tropical forests are major reservoirs of biodiversity and carbon, hosting between 20% and 40% of the species of fauna and flora of the planet, respectively [1,2]. Moreover, environmental changes in these regions are known to affect important ecosystem services, such as biodiversity, climate regulation, carbon storage, and water supply [3,4].

In the world’s largest rainforest, the Brazilian Amazon, important changes in the climate system were observed, evidenced mainly by the intensification of recurrence of extreme droughts and floods [5].

These changes are related to global climatic variations due to (1) natural processes related to sea surface temperature fluctuations, such as the Atlantic Multidecadal Oscillation (AMO), El Niño Southern Oscillation (ENSO), and the Pacific Decadal Oscillation (PDO) [5–8], or (2) anthropic interventions, related to land-use and land-cover changes [9–11]. In the last century, eight droughts occurred in the Amazon region, with an average interval of 12 years. In just the first sixteen years of the 21st century, four droughts with an average return interval of 4 years, have been identified [5]. This observed intensification in drought frequency can be a result of the effects of climate change on the hydrological cycle in the Amazon, which were predicted in several global models for the 21st century [12].

The occurrence of droughts causes significant impacts on the structure and function of Amazonian ecosystems, such as increased susceptibility of forests to fire [7,13,14], changes in forest carbon balance [15–17], and problems related to water supply [18]. Flood events, on the other hand, cause direct impacts to riverine populations, such as material loss, loss of human life, health impacts, and negative consequences for the local economy [19,20].

Some authors have found evidence of change in the occurrence of rainfall using weather stations throughout the Brazilian Amazon. Marengo [21] for example, using observational rainfall data for the period 1929–1998, found a negative trend for the entire Amazon Basin, while at the regional level, these authors have observed a negative trend in the north and a positive trend in the southern part of the Basin. Marcuzzo et al. [22] analysed 30 years of observational rainfall data from 37 weather stations located in the south of the Brazilian Amazon biome (state of Mato Grosso), and found a tendency of rainfall increase in March (wet season in the region), and a trend of reduction in June (dry season in the region). Santos et al. [23] used daily rainfall data collected from 305 weather stations between 1983 and 2012 throughout the Brazilian Amazon and found a significant increase in the number of days with precipitation above the 50% and 95% quantiles in the northeast region, and a significant reduction tendency in the number of days with precipitation above the 95% quantile in the southern region. Silva et al. [24] analysed a series of rainfall data collected by 12 weather stations in the state of Maranhão (eastern Amazon) between 1977 and 2014, finding a significant trend of increased precipitation in the ecotone region between the Amazon and the Cerrado (Brazilian Savannas) biomes and a reduction within the Amazon biome. In a recent comprehensive study, Almeida et al. [25] analysed spatially and temporally explicit rainfall data in the Brazilian Legal Amazon using 47 weather stations covering the period between 1973 and 2013 and found no trends for most stations. Nevertheless, some stations showed significant increasing trends in annual and wet season rainfall, while some presented significant decreasing trends in the dry season.

Limitations on the spatial distribution of the world's weather stations network curtail the capacity to develop a synoptic understanding of observed changes in rainfall patterns. Thus, rainfall data estimated directly by remote sensing technology or by reanalysis methods are a viable alternative to identifying changes in rainfall regime at different scales. Globally, Lau and Wu [26] used the GPCP (Global Precipitation Climatology Project; which integrate satellite and gauge estimates) and CMAP (Merged Analysis of Precipitation) precipitation products to detect trends in tropical rainfall between 1979 and 2003. This study found positive trends of heavy and light rainfall events and a negative trend in moderate events. Gu and Adler [27] used the monthly GPCP product and linear regressions to identify rainfall trends between 1979 and 2010, and found both positive and negative trends in continental areas of the tropics. Wang et al. [28], moreover, analysed the decadal trends in the annual global precipitation using the CMAP, GPCP, and National Centers for Environmental Prediction (NCEP) reanalysis data set, and found decreasing trends in the CMAP and reanalysis data and a flat trend in the GPCP data, where the decreasing trends were mainly associated with the increasing trend of low annual minimum precipitation rate in the CMAP data and high annual minimum precipitation rate in the reanalysis data. Adler et al. [29] evaluated the means, variations, and trends of global precipitation between 1976 and 2014 using the GPCP monthly rainfall product, and found variations in global precipitation, tied to ENSO (El Niño/Southern Oscillation) events, with increases during El Niños, and decreases after major volcanic eruptions, but no overall significant trend was noted

in the global precipitation mean value. Finally, Nguyen et al. [30] used approximately 33 years of PERSIANN-CDR global precipitation data and the Mann–Kendall method to identify annual rainfall trends at different scales, and demonstrated that warm climate regions exhibit decreasing rainfall trends, and at a country scale, rainfall increased in 96 countries, and decreased in others 104. In the Amazonian region, Salviano et al. [31] estimated rainfall trends for the entire Brazilian territory using the Climatic Research Unit—CRU monthly precipitation data between 1961 and 2011 applying the Mann–Kendall method, and found insignificant rainfall trends in more than 70% of the Brazilian territory in every month, on the other hand, the western Amazon showed a positive trend in the wet season (January to April) and a negative trend in the dry season (June to September). Arvor et al. [32] used three decades (1983–2014) of PERSIANN-CDR daily precipitation data to characterize rainfall patterns and trends in the Southern Amazon basin, using the Mann–Kendall method, where they identified significant trends toward a shortening of the wet season.

To expand the knowledge provided by previous research carried out in the Amazonian region [31,32], the aim of the present study was to analyse wall-to-wall data of monthly rainfall, directly retrieved by the TRMM satellite, combined with statistical methods for the detection of temporal trends to answer the following questions. (1) What are the critical years in which rainfall has deviated significantly from the last 18-years climatology (1998–2015)? (2) Are there any trends in rainfall during the period analysed? Moreover, a brief discussion on the impacts of rainfall variability on the Amazon biome is also provided.

2. Materials and Methods

2.1. Study Area

The Brazilian Legal Amazon area (Figure 1) was established in 1953 by Federal Law N° 1806, which included the states of Acre, Amapá, Amazonas, Pará, Rondônia, Roraima, Tocantins, Mato Grosso, and part of Maranhão (west of the meridian of 44° west longitude) [33]. Within this region, areas with intense deforestation activity are mainly concentrated in the region called the Arch of Deforestation, which borders the Cerrado biome (Brazilian Savannas) [34].

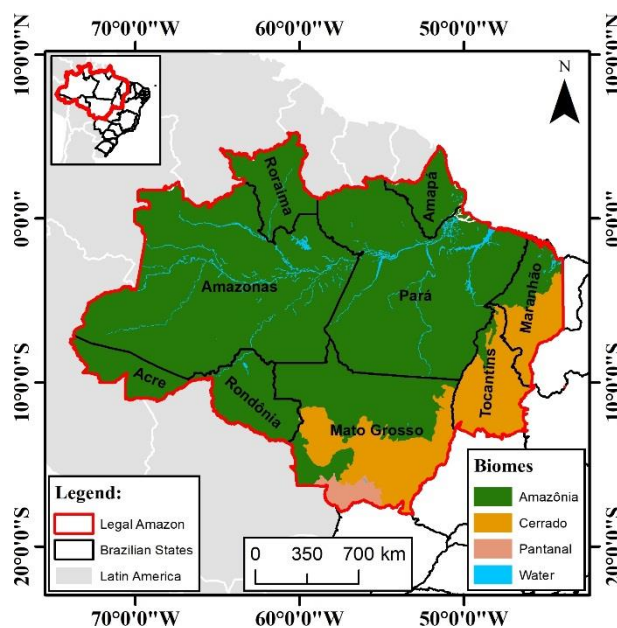


Figure 1. Location of the study area with the red line indicating the area of the Brazilian Legal Amazon, the black line are the political boundaries of Amazonian states and colours represent the different Brazilian biomes proposed by the Brazilian Institute of Geography and Statistics (IBGE) [35].

According to the Köppen classification [36], this region presents an “A” type climate, typical of tropical forests, without a cold season and average minimum temperature above 18 °C. The region can be subdivided into three subclimatic regions: rainy equatorial (“Af”), tropical monsoon (“Am”), and tropical wet and dry (“Aw”) [37]. The seasonality observed in rainfall and the rapid transition between wet and dry seasons are mainly related to the establishment of the South American Monsoon System, which is influenced by the sea surface temperature near the Equator [38]. In general, sea surface temperatures in the Pacific and in the Tropical Atlantic control intra- and interannual rainfall variability in the Amazon [38].

2.2. Rainfall Data

Monthly rainfall data from 1998 to 2015 were obtained from the Tropical Rainfall Measuring Mission satellite (TRMM) product 3B43-V7. This satellite was launched in 1997 as part of a collaborative program between the National Aeronautics and Space Administration (NASA) and the Japan Aerospace Exploration Agency (JAXA).

Gridded data from the 3B43 product is available in HDF format (Hierarchical Data Format) with a spatial resolution of 0.25 by 0.25 degrees (about 27 by 27 km or 729 km²), covering the globe between latitudes 50° N to 50° S [39]. Each pixel in the data has rainfall estimates (millimetres per month) derived from TRMM sensors and other data sources [40].

This database was chosen due to its spatial and temporal resolution that allows a more detailed analysis of the Brazilian Legal Amazon, totalling 6614 pixels. In addition, validations performed for the Amazon region showed a significant high correlation and agreement between the data estimated by the product and those observed in the field by rainfall gauges [14,41,42].

2.3. Methods

The analyses were first performed for the annual and monthly average of all pixels in our study area. To identify the spatial distribution of trends, pixel-by-pixel analyses were performed. For each pixel in the study area, the values of monthly and annual (sum of monthly rainfall values) rainfall were extracted for each year, and then the trends were quantified.

All anomalies and trend analyses were implemented in the statistical software R (version 3.4.4) [43]. The trend analyses were performed through the “Water Quality (wq)” package (version 0.4.8) using the “mannKen” and “seaKen” functions [44], for traditional and seasonal Mann–Kendall trend tests, respectively. Simultaneously the package performs the Sen’s Slope estimator. A significance level of 95% was adopted for all analyses ($p \leq 0.05$). Below, all statistical approaches are detailed.

2.3.1. Statistical Analysis of Rainfall Anomalies

To investigate the amount of rainfall for each month in relation to the average (1998–2015), standard deviation normalized precipitation anomalies were calculated (Equation (1)) [14]. Previous studies have used this methodology to identify anomalies in historical series of environmental data, such as rainfall, fires, vegetation indices, and solar radiation [14,45,46].

$$X_{Anomaly} = \frac{(X_i - \bar{X}_{1998-2015})}{\sigma_{1998-2015}} \quad (1)$$

where, X_i is the month of the year under analysis, \bar{X} the monthly average of the series 1998–2015, and σ is the standard deviation of the temporal series. Significant anomalies (95% confidence interval) were considered to be less than or equal to -1.96 and greater than or equal to 1.96 standard deviations [45].

The average (\bar{X}) and the standard deviation (σ) were calculated according to Equations (2) and (3), respectively.

$$\sigma = \sqrt{\frac{\sum_{i=1}^n (x_i - \bar{x})^2}{n}} \quad (2)$$

$$\bar{X} = \frac{\sum_{i=1}^n (x_i)}{n} \quad (3)$$

where, x_i is the series data, \bar{X} is the arithmetic mean and n is the number of observations.

2.3.2. Statistical Analysis of Rainfall Trends

The significance of trends were analysed using the Mann–Kendall test [47,48], and the magnitude of changes were quantified using the Sen's Slope estimator [49]. These two nonparametric methods do not require that the data are in conformity with a specific distribution, they are less sensitive to outlier values, and are widely used for quantifying temporal trends in time series of environmental data [50–59].

Mann–Kendall Test

In the Mann–Kendall approach, it is tested whether the observations of a given time series (X_1, X_2, \dots, X_n) are independent and identically distributed. For this, the hypotheses considered are H_0 , which states that observations are independent and identically distributed (there is no trend); and H_1 , which states that observations have a monotonic trend in time (there is a trend). Regarding H_0 , the S statistic is given by Equation (4):

$$S = \sum_{k=1}^{n-1} \sum_{j=k+1}^n \text{sign}(x_j - x_k) \quad (4)$$

where n is the number of points in the series and x represents the measurements in time; i and j are time indices, with $i \neq j$, and sign (Equation (5)) defined as:

$$\text{sign}(x) = \begin{cases} 1, & \text{if } x > 0 \\ 0, & \text{if } x = 0 \\ -1, & \text{if } x < 0 \end{cases} \quad (5)$$

The positive values of S (Equation (4)) indicate positive trends over time and negative values indicate a negative trend.

In addition, it is necessary to calculate the probability associated with S and the sample size n to define the significance of the trends. Then, for $n > 10$, a normal approximation for the Mann–Kendall test is considered. Thus, the variance of S can be given by Equation (6):

$$\text{Var}(S) = \frac{n(n-1)(2n-1) \sum_{j=1}^p t_j(t_j-1)(2t_j+5)}{18} \quad (6)$$

where, p is the number of groups with equal values in the time series and t_j is the number of data with equal values in each group j .

If S is normally distributed, with zero mean and variance given by $\text{Var}(S)$, it is possible to test whether a positive or negative trend is significantly different from zero. For S to be significant and different from zero, H_0 should be rejected considering the level of significance adopted, pointing to the existence of a trend in the time series, thus accepting H_1 .

In addition, the seasonal Mann–Kendall test [60] was applied. This test consists of performing the traditional Mann–Kendall trend test on each of the seasons separately and subsequently combining

the results of all seasons into a single metric [61]. For example, for monthly seasons, each month is analysed separately and no analysis is performed across season boundaries. In other words, the seasonal Mann–Kendall statistic is simply the sum of individual Kendall' statistics for each of the months analysed [61]. More detail can be found in Hirsch et al. and Helsel and Frans works [60,61].

Sen's Slope Estimator

After identifying trends in the time series, it is also important to estimate their magnitude. In most of the methods used for this purpose, the normality of the data is a prerequisite, being highly sensitive to outliers. To overcome this limitation, a nonparametric and robust method was developed by Sen [62] to estimate the magnitude of trends in time series.

The Sen statistic is given by the median of the slopes of each pair of points in the data set [62]. To calculate the Sen's Slope Estimator (Q), the data is ranked in ascending order, as a function of time, and then Equation (7) is applied.

$$Q = \text{Median} \left\{ \left[\left(\frac{x_i - x_j}{i - j} \right)_{j=1}^{j=n-1} \right]_{i=j+1}^{i=n} \right\} \quad (7)$$

where x_i and x_j are pairs at given times i and j ($j > i$), respectively.

3. Results and Discussion

3.1. Rainfall Anomalies Between 1998 and 2015

Figure 2 shows the anomalies of monthly rainfall averages over the Brazilian Legal Amazon from 1998 to 2015. Significant positive anomalies were identified in 1999 (2.09σ in September), 2000 (2.79σ in July and 2.22σ in September), 2004 (2.06σ in August), 2009 (2.08σ in April and 2.56σ in July), and 2013 (2.05σ in November). The anomalies observed in 1999 and 2009 are associated with extreme flood events in these years [5], related to the La Niña phenomenon in the year 1999 [19,63–67] and the warming in the tropical South Atlantic (TSA) in the year 2009 [68–71].

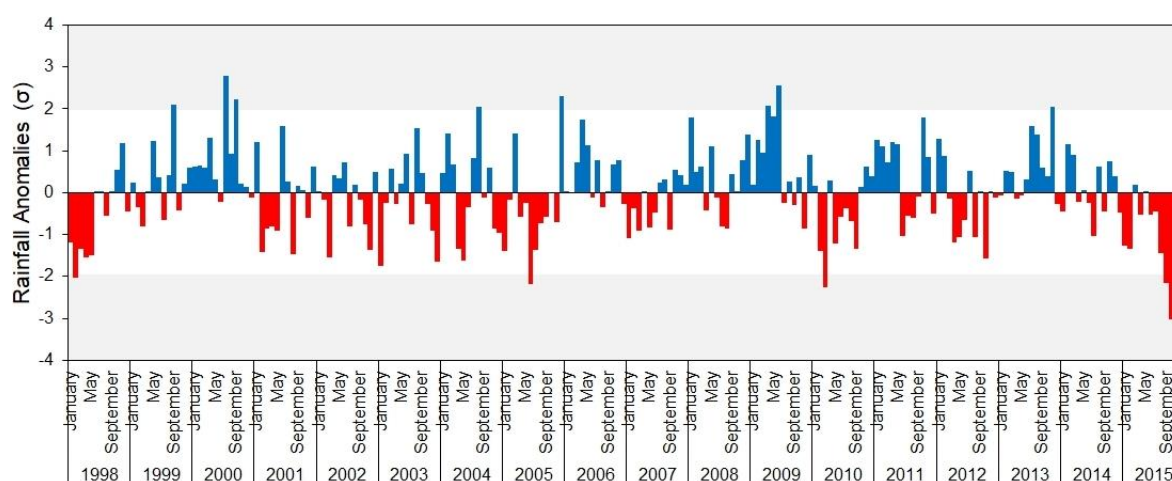


Figure 2. Regional monthly rainfall anomalies. The shaded area represents the significant positive (blue bars) and negative anomalies (red bars). The anomalies were calculated using the monthly average of all the pixels in the Brazilian Legal Amazon.

Significant negative anomalies were also identified in the years 1998 (-2.02σ in January), 2005 (-2.17σ in June), 2010 (-2.25σ in March), and 2015 (-2.16σ in September, -3.04σ in October, -2.15σ in November, and -2.04σ in December). The negative anomalies observed in those years were associated with extreme droughts in the Amazon region, mainly caused by (i) the El Niño-Southern Oscillation

(ENSO), which is linked to the warm conditions in the tropical Pacific, (ii) the anomalies in sea surface temperature (SST) of the tropical north Atlantic ocean, or by (iii) a combination of both [19]. The droughts of 1998 [66,72–75] and 2010 [66,74,76], for example, were linked to the combination of the El Niño and the warming of the Tropical North Atlantic (TNA) [7,14]. However, the 2005 drought [14,66,73,74,77–79] was mainly associated with the TNA warming, while the 2015 drought was related to a strong El Niño event [7,80]. Overall, 2015 had the lowest ever rainfall volumes during the 1998–2015 period. Significant negative anomalies between September and December 2015 were also preceded by negative anomalies, though not significant. These results suggest that the year 2015 was the driest of the 21st century in the Brazilian Legal Amazon. The year 2015, unlike other drought years, had the highest number of consecutive months with negative rainfall anomalies, perhaps due to simultaneous development of anomalous warming of the equatorial and eastern tropical north Pacific and the tropical north Atlantic oceans [7].

3.2. Spatiotemporal Rainfall Trends Between 1998 and 2015

The results of the Mann–Kendall test for the annual rainfall average over the Amazon region showed no significant trends between 1998 and 2015 ($SS = 4.18 \text{ mm year}^{-1}$ and $p = 0.82$). Confirming this result, the seasonal Mann–Kendall test showed no significant trends ($SS = -0.17 \text{ mm month}^{-1}$ and $p = 0.56$). The average monthly values of eleven out of the twelve months analysed did not show any significant trends (Table 1). September was the only month that exhibited a significant negative trend (Table 1).

Table 1. Monthly trends of average rainfall values between 1998 and 2015. The shaded months represent the dry season in the Amazon region (mean monthly precipitation less than 100 mm) [66].

Month	Sen Slope (mm month^{-1})	p
January	−0.18	1.00
February	2.13	0.11
March	1.64	0.19
April	0.47	0.76
May	0.23	0.88
June	−0.64	0.09
July	−0.23	0.45
August	−0.48	0.45
September	−2.01	0.05
October	0.24	0.71
November	0.69	0.71
December	−2.07	0.29

Although not significant, the monthly trends corroborate with the results from Silva et al. [24], who analysed rainfall gauges between 1977 and 2014 for the eastern flank of the Legal Amazon. These authors found evidence that the rainy season was becoming wetter and the dry season drier throughout the years. Similar evidence was found by Almeida et al. [25], by analysing 47 meteorological stations along the Brazilian Amazon. Marengo et al. [66], analysing a rainfall time series between 1951 and 2010 in southwest Amazon, found an increase in the length of the dry season, which is normally observed between May and September.

By analysing the local annual trends, pixel-by-pixel (Figure 3a), our results show significant negative and positive trends ($p \leq 0.05$) throughout the Brazilian Legal Amazon. Negative trends had Sen's Slope values up to $-64.92 \text{ mm year}^{-1}$, mainly located in the north of the states Rondônia, Roraima, and Maranhão, and in the southern part of the Amazonas state. Positive trends were identified in central (southwest of the Pará state), west (especially to the west and southwest of the state of Amazonas and east of the state of Pará), and to the west and southwest of the state of Amazonas, with values of Sen's Slope reaching up to $49.23 \text{ mm year}^{-1}$. No rainfall trends were observed for most of the Brazilian Legal Amazon (92.3%; 4,450,342 km^2). However, 4.2% (202,507 km^2) of the area

had significant negative trends ($p \leq 0.05$), and 3.5% (168,756 km²) had significant positive trends ($p \leq 0.05$). The pixel-by-pixel seasonal Man–Kandel trend test (Figure 3b) showed similar spatial pattern to the local annual trends (Figure 3a), were no rainfall trends observed in 82.3% (3,968,182 km²) of the Brazilian Legal Amazon, 11.9% (573,771 km²) had significant negative trends ($p \leq 0.05$), and 5.8% (279,653 km²) had significant positive trends ($p \leq 0.05$). More than half of the significant trends found with the two tests were negative.

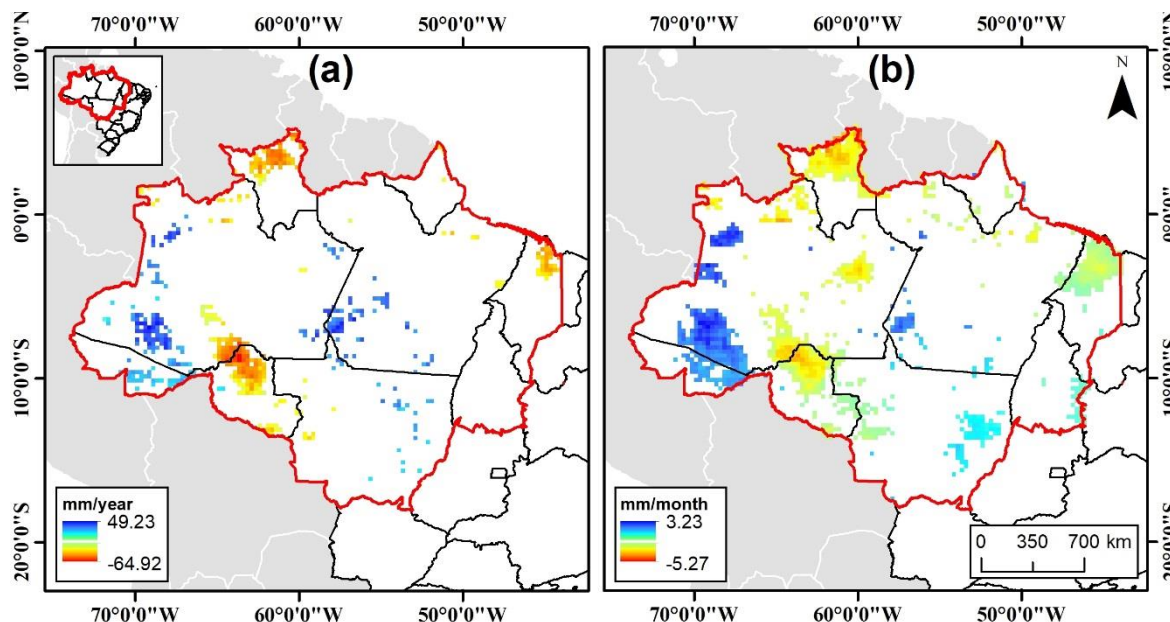


Figure 3. Spatial distribution of significant annual rainfall trends (Sen's slope; $p \leq 0.05$). Positive trends, indicating an increase in rainfall, are displayed in blue and negative trends, indicating a decrease in rainfall, are in red. (a) Annual rainfall trends and (b) seasonal rainfall trends.

The analysis of pixel-by-pixel monthly rainfall trends (Figure 4) showed similar patterns to the annual and seasonal analysis (Figure 3), with significant positive and negative rainfall trends clustered in few Amazonian regions. Significant negative trends (Sen's Slope up to $-21 \text{ mm month}^{-1}$) occurred in the north of the states of Rondônia, Roraima, and Maranhão, in most of the analysed months. Negative trends observed in September covered a large area throughout the central region of the Amazon. Significant positive trends (Sen's Slope up to 18 mm month^{-1}) were observed mainly in western Amazonas, especially in the months of January, February, March, and December. It is also important to highlight the positive trends observed in April in the eastern region of the state of Mato Grosso.

Table 2 shows the proportion of significant negative and positive rainfall trends, as well as areas with no trend. On average, no trends were observed in 95% (4,580,526 km²) of the analysed pixels, ranging from 83.99% (4,049,667 km²) in September to 97.78% (4,714,566 km²) in May. On average 3.4% (163,935 km²) of the area had significant negative trends, ranging from 0.48% (23,144 km²) in May to 15.97% (770,010 km²) in September. Moreover, the analysis showed that on average 2.24% (108,004 km²) of the area had significant positive trends, ranging from 0.05% (2411 km²) in September to 6.27% (302,315 km²) in March.

The spatial patterns observed in the annual and monthly trend analyses indicate that the recent increase in extreme drought and flood events, between 1998 and 2015 in the Amazon region, can be affected by regional rainfall patterns.

Table 2. Proportion of pixels with no tendency and with negative and positive significant trends over the months. The shaded months represent the dry season in the Amazon region (mean monthly precipitation less than 100 mm) [66].

Month	No Trend (%)	Negative Trend (%)	Positive Trend (%)
January	95.19	1.22	3.58
February	95.71	1.06	3.24
March	92.88	0.85	6.27
April	92.36	2.13	5.50
May	97.78	0.48	1.74
June	93.48	3.92	2.60
July	97.11	2.45	0.44
August	95.45	4.46	0.09
September	83.99	15.97	0.05
October	97.34	2.07	0.59
November	97.78	1.15	1.07
December	93.23	5.03	1.74

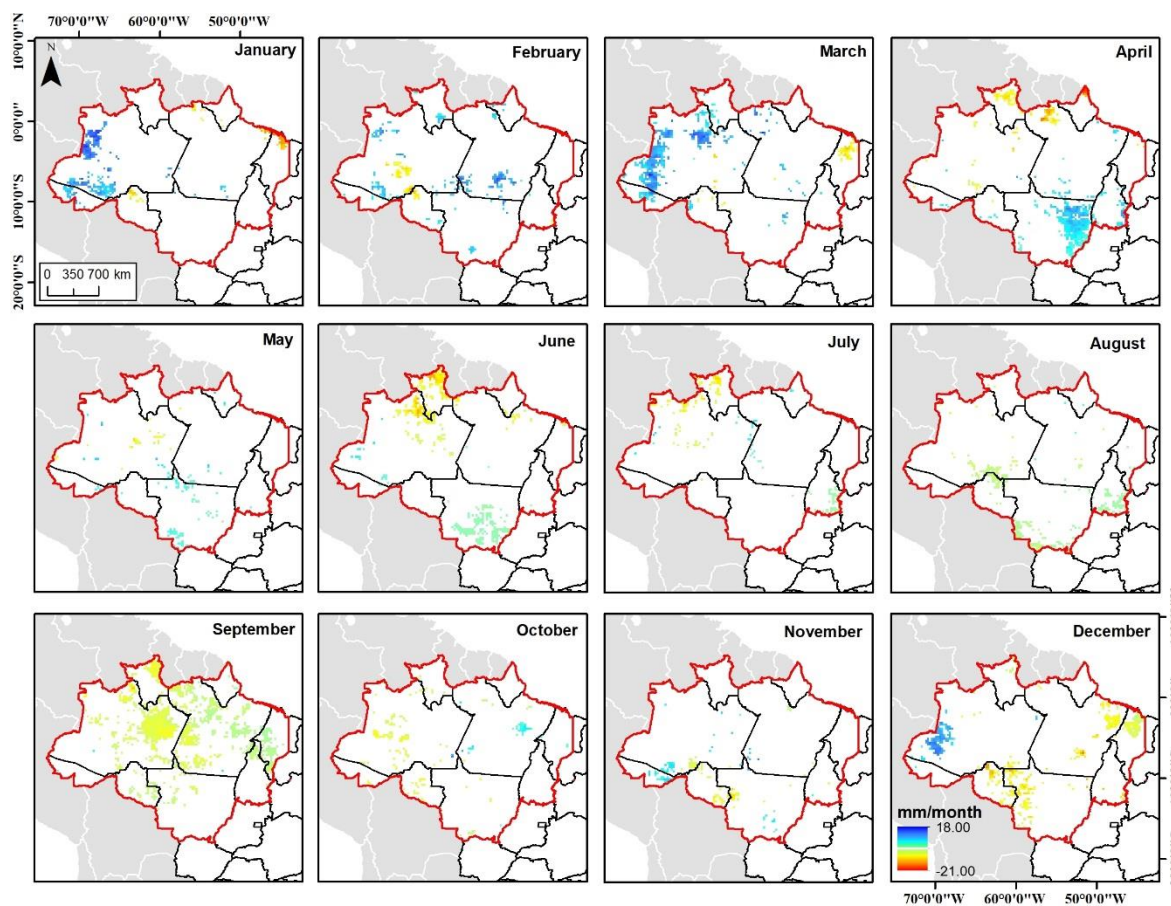


Figure 4. Spatial distribution of significant monthly rainfall trends (Sen’s slope; $p \leq 0.05$). The positive trends are in blue and the negative trends are in red.

Areas with rainfall reduction trends in the north of Maranhão and Roraima states, are visually overlapping the areas with the values of negative rainfall anomalies reported for the droughts of 1998, 2005, 2010, and 2015 [7,14,46,76,80], as well as regions where rainfall is reduced following the increase of the multivariated El Niño Index (MEI) [7,81]. However, the large area (~58,320 km²) with pixel-by-pixel negative rainfall trends in the north of Rondônia state (an old-frontier of deforestation [82]) corresponds to an area where ocean warming does not alter the rainfall patterns in the Amazon [7]. Thus, these results can be related to local hydroclimatic changes due to deforestation, corroborating previous

works [11,83,84]. It is also important to highlight that areas with a decreasing rainfall trend may be also related to the release of aerosols due to the intensification of fires in highly anthropised areas [85,86].

On the other hand, regions with an increasing rainfall trend are related to areas not affected by droughts that had positive anomalies during the droughts of 1998, 2005, 2010, and 2015, and possibly in years not reported in the literature. These patterns highlight the fact that rainfall and their anomalies are heterogeneous in space and time throughout the Amazon, depending on large-scale circulation variations and different configurations of land cover. While ENSO and PDO cause negative anomalies in the northern and central regions of the Amazon, the variations in the Tropical Atlantic SST are responsible for negative rainfall anomalies mainly in the western flank of the studied region [5,7,19].

Patterns of monthly trends found here (both positive and negative), differ from the results of Salviano et al. [31]; they used CRU rainfall data between 1961 and 2011 to analyse the spatial monthly rainfall trends over the Brazilian territory. For every month, there was no observed spatial overlap between the results found here and those reported previously [31]. On the other hand, our results are in agreement with the patterns of annual negative trends found by Arvor et al. [32], which analysed three decades (1983–2014) of PERSIANN-CDR daily precipitation data in South Amazon. Although not significant, the results of Arvor et al. [32] were consistent with negative annual trend patterns found here for Amazonas, Roraima, and Mato Grosso states. These differences and convergences between results, demonstrates that the patterns revealed here are related to recent rainfall variability and not to long-term rainfall variations.

3.3. Potential Impacts of Rainfall Variability

The patterns identified in the present study are critical because of their association with regional patterns of floods and droughts in the Amazon, with direct consequences for ecosystems and human populations. Extreme flood events are reported to have several impacts on the riverine populations of the Amazon, both in rural and urban areas [19]. The flooding of houses tends to cause loss of life and property, including those who are the most vulnerable (children and elderly) [20,87]. Furthermore, flooding of schools and hospitals is responsible for the disruption of basic services to the population [20,87]. Impacts on health are also common during flood events. Increased incidence of leptospirosis, caused by the dilution of urine from rats during floods, has been recorded during flood events [20,87]. Moreover, extreme floods have a direct impact on population mobility, affecting the functioning of towns by impairing the supply of food in the affected regions, and consequently impacting the local economy [19,20,87].

Vegetation in the Amazon can be sensitive to variations in rainfall patterns [88]. Droughts may increase the susceptibility of vegetation to fire, resulting in a greater occurrence of wildfires [7,13,14,89]. In addition, repeated droughts can lead to tree mortality, decreasing the stocks of above-ground biomass and altering local species composition [15,90,91]. Carbon emissions in the Amazon region increased from 0.24 Pg C year⁻¹ to 0.46 Pg C year⁻¹ in drought years, due to the combined effect of deforestation, fire, and forest mortality [17]. The droughts also can reduce vegetation's ability to absorb carbon [16]. Moreover, large-scale transport of atmospheric aerosols from fires during drought years can have negative impact on human health [92], airport operations, and other socioeconomic activities [93,94].

Areas with an observed rainfall reduction found in the state of Maranhão overlap an important wetland, called “Baixada Maranhense”, an Environmental Protection Area classified as a priority site by the Ramsar Convention [95]. The functional stability of these areas are strongly dependent on the rainfall regime, therefore, a reduction in rainfall input can adversely affect the natural ecosystems, and consequently the local population, which is economically dependent on this area [96–98].

Changes in rainfall patterns may also affect leaf phenological patterns, which is an important limiting factor for the growth of new leaves [99]. Thus, continuous areas of old-growth forests in the south and east of Amazonas, and north of Roraima may be negatively affected by the continuous reduction of rainfall observed between 1998 and 2015 (Figure A1).

4. Final Considerations

The findings presented here represent an important contribution to the understanding of the recent spatial pattern of rainfall changes in the Brazilian Amazon between 1998 and 2015. The pixel-by-pixel positive and negative rainfall trends presented here have not been reported previously in the literature. In the Amazon, previous studies have projected the possibility of a drier climate with more frequent extreme drought events for the 21st century [12,100]. These projections were confirmed by recent observational studies [5,7,66,80]. Although no significant trends were found for annual and most of the monthly precipitation averages, significant local trends (pixel-by-pixel) found here suggest that rainfall changes are associated with recent extreme droughts and floods events that hit the Brazilian Amazon.

Finally, results presented here provide a methodological baseline for supporting new studies aiming at quantifying trends in time-series of environmental and climatological datasets. The proposed methodology is easily applicable to other datasets and areas of study.

Author Contributions: C.H.L.S.J. led the design of the experiment and performed data analysis. C.H.L.S.J., C.T.A., J.R.N.S., L.O.A., L.E.O.C.A., and F.B.S. interpreted the results. C.H.L.S.J. and C.T.A. wrote the paper with significant contributions from all authors.

Funding: This research was funded by the Brazilian Federal Agency for Support and Evaluation of Graduate Education (CAPES), the National Council for Scientific and Technological Development (CNPq) and the Maranhão Research Foundation (FAPEMA).

Acknowledgments: We gratefully acknowledge the Brazilian Federal Agency for Support and Evaluation of Graduate Education (CAPES), the National Council for Scientific and Technological Development (CNPq) and the Maranhão Research Foundation (FAPEMA) agencies for providing research fellowships. L.O.A. and L.E.O.C. acknowledge the productivity scholarship from CNPq (grants numbers 309247/2016-0 and 305054/2016-3). We thank the editors and the anonymous reviewers for their constructive comments, which helped us to improve the paper.

Conflicts of Interest: The authors declare no conflicts of interest.

Appendix A

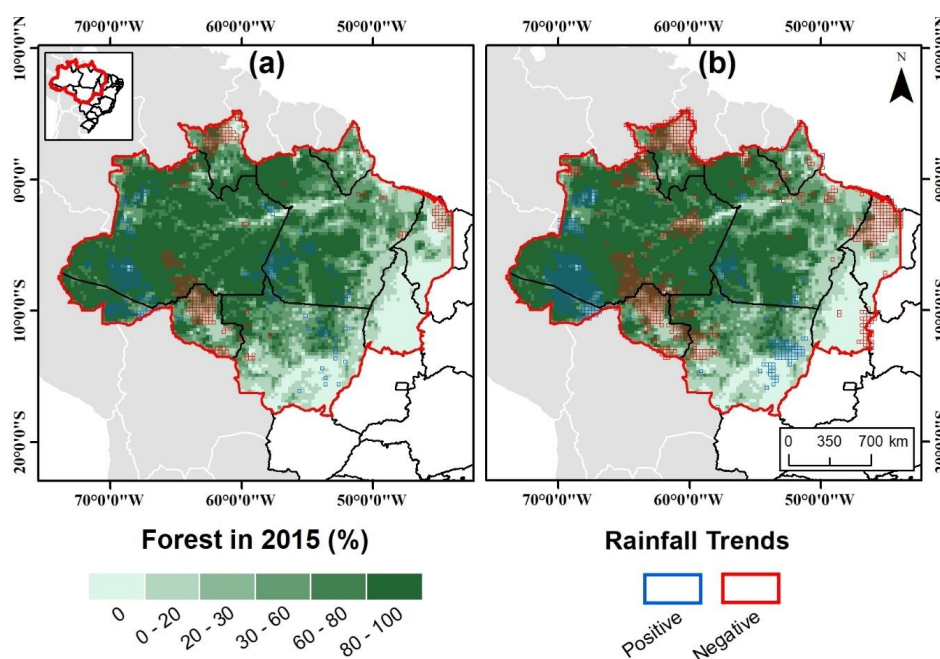


Figure A1. Spatial distribution of the old-growth forest in the study area for the year 2015 from the forest mask of the PRODES/INPE Project [101]. Forest areas were calculated as percentage in 27 by 27km cells (spatial resolution similar to Tropical Rainfall Measuring Mission (TRMM) satellite data). (a) Annual rainfall trends and (b) seasonal rainfall trends.

References

1. Myers, N. Tropical forests: Present status and future outlook. *Clim. Chang.* **1991**, *19*, 3–32. [[CrossRef](#)]
2. Sullivan, M.J.P.; Talbot, J.; Lewis, S.L.; Phillips, O.L.; Qie, L.; Begne, S.K.; Chave, J.; Cuni-Sanchez, A.; Hubau, W.; Lopez-Gonzalez, G.; et al. Diversity and carbon storage across the tropical forest biome. *Sci. Rep.* **2017**, *7*, 39102. [[CrossRef](#)] [[PubMed](#)]
3. Foley, J.A. Global Consequences of Land Use. *Science* **2005**, *309*, 570–574. [[CrossRef](#)] [[PubMed](#)]
4. Baccini, A.; Walker, W.; Carvalho, L.; Farina, M.; Sulla-Menashe, D.; Houghton, R.A. Tropical forests are a net carbon source based on aboveground measurements of gain and loss. *Science* **2017**, *358*, 230–234. [[CrossRef](#)] [[PubMed](#)]
5. Marengo, J.A.; Espinoza, J.C. Extreme seasonal droughts and floods in Amazonia: Causes, trends and impacts. *Int. J. Climatol.* **2016**, *36*, 1033–1050. [[CrossRef](#)]
6. Sorí, R.; Marengo, J.; Nieto, R.; Drumond, A.; Gimeno, L. The Atmospheric Branch of the Hydrological Cycle over the Negro and Madeira River Basins in the Amazon Region. *Water* **2018**, *10*, 738. [[CrossRef](#)]
7. Aragão, L.E.O.C.; Anderson, L.O.; Fonseca, M.G.; Rosan, T.M.; Vedovato, L.B.; Wagner, F.H.; Silva, C.V.J.; Silva, C.H.L., Jr.; Arai, E.; Aguiar, A.P.; et al. 21st Century drought-related fires counteract the decline of Amazon deforestation carbon emissions. *Nat. Commun.* **2018**, *9*, 536. [[CrossRef](#)] [[PubMed](#)]
8. Mantua, N.J.; Hare, S.R.; Zhang, Y.; Wallace, J.M.; Francis, R.C. A Pacific Interdecadal Climate Oscillation with Impacts on Salmon Production. *Bull. Am. Meteorol. Soc.* **1997**, *78*, 1069–1079. [[CrossRef](#)]
9. Nobre, C.; Sampaio, G.; Salazar, L. Mudanças climáticas e Amazônia. *Cienc. Cult.* **2007**, *59*, 22–27.
10. Llopart, M.; Reboita, M.; Coppola, E.; Giorgi, F.; da Rocha, R.; de Souza, D. Land Use Change over the Amazon Forest and Its Impact on the Local Climate. *Water* **2018**, *10*, 149. [[CrossRef](#)]
11. Spracklen, D.V.; Garcia-Carreras, L. The impact of Amazonian deforestation on Amazon basin rainfall. *Geophys. Res. Lett.* **2015**, *42*, 9546–9552. [[CrossRef](#)]
12. Malhi, Y.; Roberts, J.T.; Betts, R.A.; Killeen, T.J.; Li, W.; Nobre, C.A. Climate Change, Deforestation, and the Fate of the Amazon. *Science* **2008**, *319*, 169–172. [[CrossRef](#)] [[PubMed](#)]
13. Nepstad, D.; Lefebvre, P.; Lopes da Silva, U.; Tomasella, J.; Schlesinger, P.; Solorzano, L.; Moutinho, P.; Ray, D.; Guerreira Benito, J. Amazon drought and its implications for forest flammability and tree growth: A basin-wide analysis. *Glob. Chang. Biol.* **2004**, *10*, 704–717. [[CrossRef](#)]
14. Aragão, L.E.O.C.; Malhi, Y.; Roman-Cuesta, R.M.; Saatchi, S.; Anderson, L.O.; Shimabukuro, Y.E. Spatial patterns and fire response of recent Amazonian droughts. *Geophys. Res. Lett.* **2007**, *34*, L07701. [[CrossRef](#)]
15. Phillips, O.L.; Aragao, L.E.O.C.; Lewis, S.L.; Fisher, J.B.; Lloyd, J.; Lopez-Gonzalez, G.; Malhi, Y.; Monteagudo, A.; Peacock, J.; Quesada, C.A.; et al. Drought Sensitivity of the Amazon Rainforest. *Science* **2009**, *323*, 1344–1347. [[CrossRef](#)] [[PubMed](#)]
16. Brienen, R.J.W.; Phillips, O.L.; Feldpausch, T.R.; Gloor, E.; Baker, T.R.; Lloyd, J.; Lopez-Gonzalez, G.; Monteagudo-Mendoza, A.; Malhi, Y.; Lewis, S.L.; et al. Long-term decline of the Amazon carbon sink. *Nature* **2015**, *519*, 344–348. [[CrossRef](#)] [[PubMed](#)]
17. Aragão, L.E.O.C.; Poulter, B.; Barlow, J.B.; Anderson, L.O.; Malhi, Y.; Saatchi, S.; Phillips, O.L.; Gloor, E. Environmental change and the carbon balance of Amazonian forests. *Biol. Rev.* **2014**, *89*, 913–931. [[CrossRef](#)] [[PubMed](#)]
18. Jinno, K. Risk Assessment of a Water Supply System during Drought. *Int. J. Water Resour. Dev.* **1995**, *11*, 185–204. [[CrossRef](#)]
19. Marengo, J.A.; Borma, L.S.; Rodriguez, D.A.; Pinho, P.; Soares, W.R.; Alves, L.M. Recent Extremes of Drought and Flooding in Amazonia: Vulnerabilities and Human Adaptation. *Am. J. Clim. Chang.* **2013**, *2*, 87–96. [[CrossRef](#)]
20. Santos, L.B.L.; Carvalho, T.; Anderson, L.O.; Rudorff, C.M.; Marchezini, V.; Londe, L.R.; Saito, S.M. An RS-GIS-Based Comprehensive Impact Assessment of Floods—A Case Study in Madeira River, Western Brazilian Amazon. *IEEE Geosci. Remote Sens. Lett.* **2017**, *14*, 1614–1617. [[CrossRef](#)]
21. Marengo, J.A. Interdecadal variability and trends of rainfall across the Amazon basin. *Theor. Appl. Climatol.* **2004**, *78*. [[CrossRef](#)]
22. Marcuzzo, F.F.N.; Cardoso, M.R.D.; Faria, T.G. Chuvas na Amazônia mato-grossense: Análise histórica e tendência futura. *Caminhos Geogr.* **2011**, *12*, 65–75.

23. Santos, E.B.; Lucio, P.S.; Silva, C.M.S. Análise de Tendência da Precipitação Diária na Amazônia Brasileira. *Rev. Bras. Geogr. Fís.* **2015**, *8*, 1041–1052. [[CrossRef](#)]
24. Silva, F.B.; Santos, J.R.N.; Feitosa, F.E.C.S.; Silva, I.D.C.; de Araújo, M.L.S.; Guterres, C.E.; dos Santos, J.S.; Ribeiro, C.V.; da Silva Bezerra, D.; Neres, R.L. Evidências de Mudanças Climáticas na Região de Transição Amazônia-Cerrado no Estado do Maranhão. *Rev. Bras. Meteorol.* **2016**, *31*, 330–336. [[CrossRef](#)]
25. Almeida, C.T.; Oliveira-Júnior, J.F.; Delgado, R.C.; Cubo, P.; Ramos, M.C. Spatiotemporal rainfall and temperature trends throughout the Brazilian Legal Amazon, 1973–2013. *Int. J. Climatol.* **2017**, *37*, 2013–2026. [[CrossRef](#)]
26. Lau, K.-M.; Wu, H.-T. Detecting trends in tropical rainfall characteristics, 1979–2003. *Int. J. Climatol.* **2007**, *27*, 979–988. [[CrossRef](#)]
27. Gu, G.; Adler, R.F. Interdecadal variability/long-term changes in global precipitation patterns during the past three decades: Global warming and/or pacific decadal variability? *Clim. Dyn.* **2013**, *40*, 3009–3022. [[CrossRef](#)]
28. Wang, B.; Li, X.; Huang, Y.; Zhai, G. Decadal trends of the annual amplitude of global precipitation. *Atmos. Sci. Lett.* **2016**, *17*, 96–101. [[CrossRef](#)]
29. Adler, R.F.; Gu, G.; Sapiiano, M.; Wang, J.-J.; Huffman, G.J. Global Precipitation: Means, Variations and Trends During the Satellite Era (1979–2014). *Surv. Geophys.* **2017**, *38*, 679–699. [[CrossRef](#)]
30. Nguyen, P.; Thorstensen, A.; Sorooshian, S.; Hsu, K.; Aghakouchak, A.; Ashouri, H.; Tran, H.; Braithwaite, D. Global Precipitation Trends across Spatial Scales Using Satellite Observations. *Bull. Am. Meteorol. Soc.* **2018**, *99*, 689–697. [[CrossRef](#)]
31. Salviano, M.F.; Groppo, J.D.; Pellegrino, G.Q. Análise de Tendências em Dados de Precipitação e Temperatura no Brasil. *Rev. Bras. Meteorol.* **2016**, *31*, 64–73. [[CrossRef](#)]
32. Arvor, D.; Funatsu, B.; Michot, V.; Dubreuil, V. Monitoring Rainfall Patterns in the Southern Amazon with PERSIANN-CDR Data: Long-Term Characteristics and Trends. *Remote Sens.* **2017**, *9*, 889. [[CrossRef](#)]
33. Martha Júnior, G.B.; Contini, E.; Navarro, Z. *Caracterização da Amazônia Legal e Macrotendências do Ambiente Externo*; Embrapa Estudos e Capacitação: Brasília, Brazil, 2011.
34. Caúla, R.H.; Oliveira-Júnior, J.F.; Lyra, G.B.; Delgado, R.C.; Heilbron Filho, P.F.L. Overview of fire foci causes and locations in Brazil based on meteorological satellite data from 1998 to 2011. *Environ. Earth Sci.* **2015**, *74*, 1497–1508. [[CrossRef](#)]
35. IBGE Biomas. Available online: <http://7a12.ibge.gov.br/vamos-conhecer-o-brasil/nosso-territorio/biomas> (accessed on 1 March 2017).
36. Köppen, W. Versuch einer Klassifikation der Klimate, vorzugsweise nach ihren Beziehungen zur Pflanzenwelt. *Geogr. Z.* **1900**, *6*, 593–611.
37. Bastos, T.X. *O clima da Amazônia Brasileira Segundo Koppen*; EMBRAPA-CPATU: Belém, Brazil, 1982.
38. Nobre, C.A.; Obregón, G.O.; Marengo, J.A.; Fu, R.; Poveda, G. Characteristics of Amazonian climate: Main features. In *Amazonia and Global Change*; Keller, M., Bustamante, M., Gash, J., Dias, P.S., Eds.; American Geophysical Union: Washington, DC, USA, 2009; pp. 149–162, ISBN 978-0-87590-476-4.
39. NASA. The Tropical Rainfall Measuring Mission (TRMM). Available online: <http://trmm.gsfc.nasa.gov/> (accessed on 1 January 2016).
40. Huffman, G.J.; Bolvin, D.T. TRMM and Other Data Precipitation Data Set Documentation. Available online: https://docserver.gesdisc.eosdis.nasa.gov/public/project/GPM/3B42_3B43_doc_V7.pdf (accessed on 1 April 2018).
41. De Almeida, C.T.; Delgado, R.C.; de Oliveira Junior, J.F.; Gois, G.; Cavalcanti, A.S. Avaliação das Estimativas de Precipitação do Produto 3B43-TRMM do Estado do Amazonas. *Floresta Ambiente* **2015**, *22*, 279–286. [[CrossRef](#)]
42. Santos, J.R.N.; Silva, F.B.; Silva, C.H.L., Jr.; de Araújo, M.L.S. Precisão dos dados do satélite Tropical Rainfall Measuring Mission (TRMM) na região de transição Amazônia-Cerrado no Estado do Maranhão. In Proceedings of the XVII Simpósio Brasileiro de Sensoriamento, João Pessoa, PB, Brasil, 25–29 April 2015; INPE: João Pessoa, Brasil, 2015; pp. 4807–4813.
43. R Core Team. R: A Language and Environment for Statistical Computing. R Foundation for Statistical Computing: Vienna, Austria. Available online: <https://www.r-project.org/> (accessed on 1 January 2018).
44. Jassby, A.D.; Cloern, J.E. Package ‘wq’. Available online: <https://cran.r-project.org/web/packages/wq/wq.pdf> (accessed on 19 May 2016).

45. Anderson, L.O.; Malhi, Y.; Aragão, L.E.O.C.; Ladle, R.; Arai, E.; Barbier, N.; Phillips, O. Remote sensing detection of droughts in Amazonian forest canopies. *New Phytol.* **2010**, *187*, 733–750. [[CrossRef](#)] [[PubMed](#)]
46. Saleska, S.R.; Didan, K.; Huete, A.R.; da Rocha, H.R. Amazon forests green-up during 2005 drought. *Science* **2007**, *318*, 612. [[CrossRef](#)] [[PubMed](#)]
47. Kendall, M.G. *Rank Correlation Methods*; Charles Griffin: London, UK, 1975.
48. Mann, H.B. Nonparametric Tests Against Trend. *Econometrica* **1945**, *13*, 245–259. [[CrossRef](#)]
49. Salmi, T.; Maatta, A.; Anttila, P.; Ruoho-Airola, T.; Amnell, T. *Detecting Trends of Annual Values of Atmospheric Pollutants by the Mann-Kendall Test and Sen's Solpe Estimates the Excel Template Application MAKESENS*; Publications on Air Quality; Finish Meteorological Institute: Helsinki, Finland, 2002.
50. Yu, P.-S.; Yang, T.-C.; Wu, C.-K. Impact of climate change on water resources in southern Taiwan. *J. Hydrol.* **2002**, *260*, 161–175. [[CrossRef](#)]
51. Hipel, K.W.; McLeod, A.I. *Time Series Modelling of Water Resources and Environmental Systems*, 1st ed.; Elsevier: Amsterdam, The Netherlands, 2005; ISBN 9780080870366.
52. Chandler, R.E.; Scott, E.M. (Eds.) *Statistical Methods for Trend Detection and Analysis in the Environmental Sciences*; John Wiley & Sons, Ltd: Chichester, UK, 2011; ISBN 9781119991571.
53. Wilks, D. (Ed.) *Statistical Methods in the Atmospheric Sciences*, 3rd ed.; Academic Press: Burlington, MA, USA, 2011; ISBN 9780123850232.
54. Zilli, M.T.; Carvalho, L.M.V.; Liebmann, B.; Silva Dias, M.A. A comprehensive analysis of trends in extreme precipitation over southeastern coast of Brazil. *Int. J. Climatol.* **2017**, *37*, 2269–2279. [[CrossRef](#)]
55. Xu, Z.X.; Takeuchi, K.; Ishidaira, H. Monotonic trend and step changes in Japanese precipitation. *J. Hydrol.* **2003**. [[CrossRef](#)]
56. Partal, T.; Kahya, E. Trend analysis in Turkish precipitation data. *Hydrol. Process.* **2006**, *20*, 2011–2026. [[CrossRef](#)]
57. Gocic, M.; Trajkovic, S. Analysis of changes in meteorological variables using Mann-Kendall and Sen's slope estimator statistical tests in Serbia. *Glob. Planet. Chang.* **2013**, *100*, 172–182. [[CrossRef](#)]
58. Sharma, D.; Babel, M.S. Trends in extreme rainfall and temperature indices in the western Thailand. *Int. J. Climatol.* **2014**, *34*, 2393–2407. [[CrossRef](#)]
59. Wu, C.; Huang, G.; Yu, H.; Chen, Z.; Ma, J. Spatial and temporal distributions of trends in climate extremes of the Feilaixia catchment in the upstream area of the Beijiang River Basin, South China. *Int. J. Climatol.* **2014**, *34*, 3161–3178. [[CrossRef](#)]
60. Hirsch, R.M.; Slack, J.R.; Smith, R.A. Techniques of trend analysis for monthly water quality data. *Water Resour. Res.* **1982**. [[CrossRef](#)]
61. Helsel, D.R.; Frans, L.M. Regional Kendall Test for Trend. *Environ. Sci. Technol.* **2006**, *40*, 4066–4073. [[CrossRef](#)] [[PubMed](#)]
62. Sen, P.K. Estimates of the Regression Coefficient Based on Kendall's Tau. *J. Am. Stat. Assoc.* **1968**, *63*, 1379. [[CrossRef](#)]
63. Satyamurty, P.; Da Costa, C.P.W.; Manzi, A.O.; Candido, L.A. A quick look at the 2012 record flood in the Amazon Basin. *Geophys. Res. Lett.* **2013**, *40*, 1396–1401. [[CrossRef](#)]
64. Espinoza, J.C.; Ronchail, J.; Frappart, F.; Lavado, W.; Santini, W.; Guyot, J.L. The Major Floods in the Amazonas River and Tributaries (Western Amazon Basin) during the 1970–2012 Period: A Focus on the 2012 Flood. *J. Hydrometeorol.* **2013**, *14*, 1000–1008. [[CrossRef](#)]
65. Marengo, J.A.; Alves, L.M.; Soares, W.R.; Rodriguez, D.A.; Camargo, H.; Riveros, M.P.; Pabló, A.D. Two contrasting severe seasonal extremes in tropical South America in 2012: Flood in Amazonia and drought in Northeast Brazil. *J. Clim.* **2013**, *26*, 9137–9154. [[CrossRef](#)]
66. Marengo, J.A.; Tomasella, J.; Alves, L.M.; Soares, W.R.; Rodriguez, D.A. The drought of 2010 in the context of historical droughts in the Amazon region. *Geophys. Res. Lett.* **2011**, *38*. [[CrossRef](#)]
67. Ronchail, J.; Guyot, J.-L.; Espinoza, J.C.; Fraizy, P.; Cochonneau, G.; De Oliveira, E.; Filizola, N.; Ordoñez, J.J. Impact of the Amazon tributaries on major flood in Óbidos. In *Climate Variability and Change—Hydrological Impacts, Proceedings of the Fifth FRIEND World Conference held at Havana, Cuba, 27 November–1 December 2006*; IAHS: Wallingford, UK, 2006; pp. 111–125.
68. Marengo, J.A.; Tomasella, J.; Soares, W.R.; Alves, L.M.; Nobre, C.A. Extreme climatic events in the Amazon basin: Climatological and Hydrological context of recent floods. *Theor. Appl. Climatol.* **2012**, *107*, 73–85. [[CrossRef](#)]

69. Filizola, N.; Latrubesse, E.M.; Fraizy, P.; Souza, R.; Guimarães, V.; Guyot, J.L. Was the 2009 flood the most hazardous or the largest ever recorded in the Amazon? *Geomorphology* **2014**, *215*, 99–105. [[CrossRef](#)]
70. Sena, J.A.; Beser de Deus, L.A.; Freitas, M.A.V.; Costa, L. Extreme Events of Droughts and Floods in Amazonia: 2005 and 2009. *Water Resour. Manag.* **2012**, *26*, 1665–1676. [[CrossRef](#)]
71. Vale, R.; Filizola, N.; Souza, R.; Schongart, J. A cheia de 2009 na Amazonia Brasileira. *Rev. Bras. Geociênc.* **2011**, *41*, 577–586. [[CrossRef](#)]
72. Sombroek, W. Spatial and Temporal Patterns of Amazon Rainfall. *AMBIO J. Hum. Environ.* **2001**, *30*, 388–396. [[CrossRef](#)]
73. Zeng, N.; Yoon, J.-H.; Marengo, J.A.; Subramaniam, A.; Nobre, C.A.; Mariotti, A.; Neelin, J.D. Causes and impacts of the 2005 Amazon drought. *Environ. Res. Lett.* **2008**, *3*, 014002. [[CrossRef](#)]
74. Espinoza, J.C.; Ronchail, J.; Guyot, J.L.; Junquas, C.; Vauchel, P.; Lavado, W.; Drapeau, G.; Pombosa, R. Climate variability and extreme drought in the upper Solimões River (western Amazon Basin): Understanding the exceptional 2010 drought. *Geophys. Res. Lett.* **2011**, *38*. [[CrossRef](#)]
75. dos Santos, S.R.Q.; Braga, C.C.; Sansigolo, C.A.; Neves, T.T.D.A.T.; dos Santos, A.P.P. Droughts in the Amazon: Identification, Characterization and Dynamical Mechanisms Associated. *Am. J. Clim. Chang.* **2017**, *6*, 425–442. [[CrossRef](#)]
76. Lewis, S.L.; Brando, P.M.; Phillips, O.L.; van der Heijden, G.M.F.; Nepstad, D. The 2010 Amazon Drought. *Science* **2011**, *331*, 554. [[CrossRef](#)] [[PubMed](#)]
77. Cox, P.M.; Harris, P.P.; Huntingford, C.; Betts, R.A.; Collins, M.; Jones, C.D.; Jupp, T.E.; Marengo, J.A.; Nobre, C.A. Increasing risk of Amazonian drought due to decreasing aerosol pollution. *Nature* **2008**, *453*, 212–215. [[CrossRef](#)] [[PubMed](#)]
78. Yoon, J.-H.; Zeng, N. An Atlantic influence on Amazon rainfall. *Clim. Dyn.* **2010**, *34*, 249–264. [[CrossRef](#)]
79. Tomasella, J.; Borma, L.S.; Marengo, J.A.; Rodriguez, D.A.; Cuartas, L.A.; Nobre, A.C.; Prado, M.C.R. The droughts of 1996–1997 and 2004–2005 in Amazonia: Hydrological response in the river main-stem. *Hydrol. Process.* **2011**, *25*, 1228–1242. [[CrossRef](#)]
80. Jiménez-Muñoz, J.C.; Mattar, C.; Barichivich, J.; Santamaria-Artigas, A.; Takahashi, K.; Malhi, Y.; Sobrino, J.A.; van der Schrier, G. Record-breaking warming and extreme drought in the Amazon rainforest during the course of El Niño 2015–2016. *Sci. Rep.* **2016**, *6*, 33130. [[CrossRef](#)] [[PubMed](#)]
81. Wolter, K.; Timlin, M.S. El Niño/Southern Oscillation behaviour since 1871 as diagnosed in an extended multivariate ENSO index (MEI.ext). *Int. J. Climatol.* **2011**, *31*, 1074–1087. [[CrossRef](#)]
82. Fearnside, P.M.; Salati, E. Explosive Deforestation in Rondônia, Brazil. *Environ. Conserv.* **1985**, *12*, 355. [[CrossRef](#)]
83. Butt, N.; de Oliveira, P.A.; Costa, M.H. Evidence that deforestation affects the onset of the rainy season in Rondonia, Brazil. *J. Geophys. Res.* **2011**, *116*, D11120. [[CrossRef](#)]
84. Khanna, J.; Medvigy, D.; Fueglistaler, S.; Walko, R. Regional dry-season climate changes due to three decades of Amazonian deforestation. *Nat. Clim. Chang.* **2017**, *7*, 200–204. [[CrossRef](#)]
85. Lin, J.C.; Matsui, T.; Pielke, R.A.; Kummerow, C. Effects of biomass-burning-derived aerosols on precipitation and clouds in the Amazon Basin: A satellite-based empirical study. *J. Geophys. Res.* **2006**, *111*, D19204. [[CrossRef](#)]
86. Gonçalves, W.A.; Machado, L.A.T.; Kirstetter, P.-E. Influence of biomass aerosol on precipitation over the Central Amazon: An observational study. *Atmos. Chem. Phys.* **2015**, *15*, 6789–6800. [[CrossRef](#)]
87. Dolman, D.I.; Brown, I.F.; Anderson, L.O.; Warner, J.F.; Marchezini, V.; Santos, G.L.P. Re-thinking socio-economic impact assessments of disasters: The 2015 flood in Rio Branco, Brazilian Amazon. *Int. J. Disaster Risk Reduct.* **2018**, *31*, 212–219. [[CrossRef](#)]
88. Hilker, T.; Lyapustin, A.I.; Tucker, C.J.; Hall, F.G.; Myneni, R.B.; Wang, Y.; Bi, J.; Mendes de Moura, Y.; Sellers, P.J. Vegetation dynamics and rainfall sensitivity of the Amazon. *Proc. Natl. Acad. Sci. USA* **2014**, *111*, 16041–16046. [[CrossRef](#)] [[PubMed](#)]
89. Silva, C.H.L., Jr.; Aragão, L.; Fonseca, M.; Almeida, C.; Vedovato, L.; Anderson, L. Deforestation-Induced Fragmentation Increases Forest Fire Occurrence in Central Brazilian Amazonia. *Forests* **2018**, *9*, 305. [[CrossRef](#)]
90. Feldpausch, T.R.; Phillips, O.L.; Brienen, R.J.W.; Gloor, E.; Lloyd, J.; Lopez-Gonzalez, G.; Monteagudo-Mendoza, A.; Malhi, Y.; Alarcón, A.; Álvarez Dávila, E.; et al. Amazon forest response to repeated droughts. *Glob. Biogeochem. Cycles* **2016**, *30*, 964–982. [[CrossRef](#)]

91. Nepstad, D.C.; Tohver, I.M.; Ray, D.; Moutinho, P.; Cardinot, G. Mortality of large trees and lianas following experimental drought in an Amazon forest. *Ecology* **2007**, *88*, 2259–2269. [[CrossRef](#)] [[PubMed](#)]
92. Smith, L.T.; Aragão, L.E.O.C.; Sabel, C.E.; Nakaya, T. Drought impacts on children's respiratory health in the Brazilian Amazon. *Sci. Rep.* **2014**, *4*, 3726. [[CrossRef](#)] [[PubMed](#)]
93. Anderson, L.O.; Trivedi, M.; Queiroz, J.; Aragão, L.; Marengo, J.A.; Young, C.; Meir, P. Counting the costs of the 2005 Amazon drought: A preliminary assessment. In *Ecosystem Services for Poverty Alleviation in Amazonia*; Meir, P., Ed.; Global Canopy Programme and University of Edinburgh: Edinburgh, UK, 2011; pp. 96–108.
94. Lathuillière, M.; Coe, M.; Castanho, A.; Graesser, J.; Johnson, M. Evaluating Water Use for Agricultural Intensification in Southern Amazonia Using the Water Footprint Sustainability Assessment. *Water* **2018**, *10*, 349. [[CrossRef](#)]
95. Ramsar. The List of Wetlands of International Importance. Available online: <https://www.ramsar.org/sites/default/files/documents/library/sitelist.pdf> (accessed on 6 August 2018).
96. Mendes, J.J.; Silva, F.B.; Galvão, A.T.F.; Junior, C.H.L.S. Geotecnologias aplicadas no mapeamento de áreas inundáveis na Baixada Maranhense. In Proceedings of the XVII Simpósio Brasileiro de Sensoriamento, João Pessoa, PB, Brasil, 25–29 April 2015; INPE: João Pessoa, Brasil, 2015; pp. 3943–3949.
97. Freire, A.; Mendes, J.; Silva, F.; Silva, C.H.L., Jr.; Lima Neto, R. O ambiente geológico-pedológico das Planícies Inundáveis do Maranhão e sua fragilidade às ações antrópicas. In Proceedings of the Safety, Health and Environment World Congress, Cubatão, Brasil, 20–23 July 2014; COPEC: Cubatão, Brasil, 2014; Volume 14, pp. 113–117.
98. Silva Junior, C.H.L.; Freire, A.T.G.; Rodrigues, T.C.S.; Viegas, J.C.; Bezerra, D.S. Dinâmica das Queimadas na Baixada Maranhense. *InterEspaço Rev. Geogr. e Interdiscip.* **2016**, *2*, 355–375. [[CrossRef](#)]
99. Wagner, F.H.; Hérault, B.; Rossi, V.; Hilker, T.; Maeda, E.E.; Sanchez, A.; Lyapustin, A.I.; Galvão, L.S.; Wang, Y.; Aragão, L.E.O.C. Climate drivers of the Amazon forest greening. *PLoS ONE* **2017**, *12*, e0180932. [[CrossRef](#)] [[PubMed](#)]
100. Li, W.; Fu, R.; Dickinson, R.E. Rainfall and its seasonality over the Amazon in the 21st century as assessed by the coupled models for the IPCC AR4. *J. Geophys. Res.* **2006**, *111*, D02111. [[CrossRef](#)]
101. INPE—Instituto Nacional de Pesquisas Espaciais Projeto Prodes: Monitoramento da Floresta Amazônica Brasileira por Satélite. Available online: <http://www.obt.inpe.br/prodes/> (accessed on 10 February 2016).



© 2018 by the authors. Licensee MDPI, Basel, Switzerland. This article is an open access article distributed under the terms and conditions of the Creative Commons Attribution (CC BY) license (<http://creativecommons.org/licenses/by/4.0/>).